Steel and Composite Structures, *Vol*. *26*, *No*. *3* (*2018*) *303-314*
DOI: https://doi.org/10.12989/scs.2018.26.3.303

Hydro-mechanical analysis of non-uniform shrinkage development and its effects on steel-concrete composite slabs

Safat Al-Deen*

School of Engineering and Information Technology, *The University of New South Wales*, *Canberra*, *Australia*

(*Received July 10, 2017, Revised October 18, 2017, Accepted November 7, 2017*)

Abstract. Drying shrinkage in concrete caused by drying and the associated decrease in moisture content is one of the most important factors influencing the long-term deflection of steel-concrete composite slabs. The presence of profiled steel decking at the bottom of the composite slab causes non-uniform drying from top and bottom of the slab resulting non-uniform drying shrinkage. In this paper, a hydro-mechanical analysis method is proposed to simulate the development of non-uniform shrinkage through the depth of the composite slab. It also demonstrates how this proposed analysis method can be used in conjunction with previously presented structural analysis model to calculate the effects of non-uniform shrinkage on the long-term deflection of the slab. The method uses concrete moisture diffusion model to simulate the non-uniform drying of composite slab. Then mechanical models are used to calculate resulting shrinkage strain from non-uniform drying and its effect on the long-term behaviour of the composite slabs. The performance of the proposed analysis method is validated against experimental data.

Keywords: hydro-mechanical analysis; composite; concrete; shrinkage; slabs; steel

1. Introduction

Use of profiled steel decking as sacrificial permanent formwork for steel-concrete composite slab construction expedites the construction process; which results in overall cost saving. This steel decking also acts as an external reinforcement of the hardened concrete slab. In this arrangement, when the steel-concrete composite slab is subjected to sagging bending, the compression is taken by the concrete, and the tension is taken by the steel decking, which makes it an efficient design. This design efficiency enables the use of smaller cross-sections, resulting in further cost saving. As a result, this form of construction has become very popular in various parts of the world. Throughout the years' extensive research have been conducted exploring various characteristics of composite slabs. Most of the research focussed on their ultimate response, e.g., Porter and Ekberg Jr. (1977), Porter (1985), Stark and Brekelmans (1990), Daniels and Crisinel (1993), Veljković (1998), Marimuthu *et al*. (2007), Lopes and Simões (2008), Eldib *et al*. (2009), Kim and Jeong (2010), Ranzi *et al*. (2013b), and on the identification of the interface properties between the concrete and the profiled steel sheeting, e.g., Airumyan *et al*. (1990), Easterling and Young (1992), Patrick and Bridge (1994), Veljkovic (1996), Crisinel and Marimon (2004), Jeong *et al*. (2005), Abdullah and Easterling (2009), Chen and Shi (2011), Chen *et al*. (2011), Seres and Dunai (2011), Ranzi *et al*. (2013b). However, use of smaller cross-section means that the serviceability behaviour of the composite slab is critical in the design of such slabs. In fact, previous studies Gholamhoseini *et al*. (2012), Gilbert *et al*. (2012), Gilbert (2013), Ranzi *et al*. (2013a), Ranzi *et al*. (2013c), Al-deen *et al*. (2015) have highlighted that long-term behaviour of concrete; particularly creep and shrinkage has a significant influence on the design of steel-concrete composite slabs. Despite its importance in conventional design, very limited research has been reported on the long-term behaviour of composite slabs (Ranzi *et al*. 2013a). In particular, most of the composite work on time effects has dealt with traditional composite T-beams (e.g., Roll 1971, Johnson 1987, Alsamsam 1991, Bradford and Gilbert 1991, Wright *et al*. 1992, Fan *et al*. 2010, Al-deen *et al*. 2011b, Al-Deen *et al*. 2012), with only a few studies devoted to composite slabs, e.g., Al-deen *et al*. (2011a), Gholamhoseini *et al*. (2012), Gilbert *et al*. (2012), Ranzi *et al*. (2013a).

There is a fundamental difference between the shrinkage behaviour of a solid concrete slab and that of a steel-concrete composite slab. In solid concrete slab, both top and the bottom surface of the slab is exposed to the atmosphere, allowing moisture in the concrete slab to egress (Fig. 1(a)). The steel decking at the lower part of steel-concrete composite slab prevents any moisture to egress into the atmosphere. As a result, concrete moisture can only egress from the top of the slab (Fig. 1(b)). This difference in drying process results in significantly different drying shrinkage behaviour between a solid concrete slab and that of a steel-concrete composite slab of same depth (Ranzi and Vrcelj 2009, Bradford 2010, Al-deen *et al*. 2011a, Gholamhoseini *et al*. 2012, Gilbert *et al*. 2012, Gilbert 2013, Ranzi *et al*. 2013a). This non-uniform shrinkage introduces an additional curvature and consequent

*Corresponding author, Ph.D. Lecturer,
E-mail: s.al-deen@unsw.edu.au

ISSN: 1229-9367 (Print), 1598-6233 (Online)

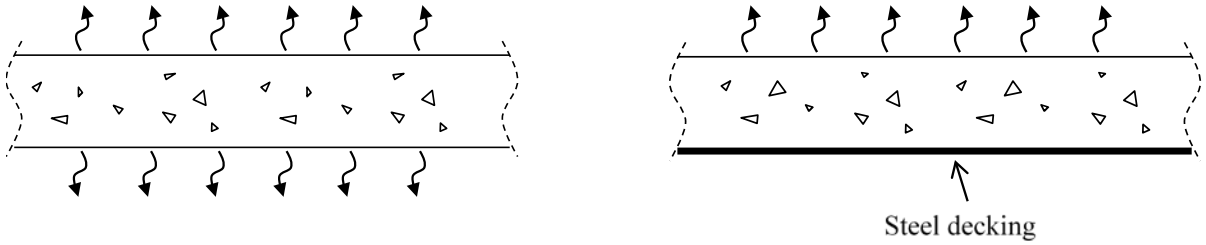

(a) Solid concrete slab; concrete moisture can egress from top and bottom of the slab

(b) Composite slab; concrete moisture can egress only from top of the slab

Fig. 1 Difference in concrete moisture egress in solid concrete and steel-concrete composite slab

deflection in composite slabs (Gholamhoseini *et al*. 2012, Gilbert *et al*. 2012, Gilbert 2013, Ranzi *et al*. 2013a, Al-deen *et al*. 2015). These papers also highlighted the importance of the non-uniform shrinkage on the long-term performance of the composite slabs.

Predicting the long-term behaviour of composite slab due to shrinkage is a two-step process. At first, the development of non-uniform shrinkage; through the depth of an equivalent slab; over time needs to be calculated. The equivalent slab is a hypothetical solid concrete slab; which has the same depth as the desired composite slab; made of same concrete and free to deform in any direction without any restraint. Additionally, it can egress moisture from the top but not from the bottom, similar to a composite slab. In the next step, the structural response of the slab due to this predicted non-uniform shrinkage is calculated. Models capable of describing the structural response of the composite slab due to non-uniform shrinkage (second part of the overall process), including the interaction between the steel sheeting and the concrete, are well documented in the available literature (Ranzi *et al*. 2013a, Al-deen and Ranzi 2015, Al-deen *et al*. 2015). However, there is currently no mathematical model, capable of predicting the development of non-uniform shrinkage through the depth of the composite slab (first part of the overall process), available in the literature. The existing design guidelines such as (AS2327.1 2003, Eurocode 4 2004) have proposed mathematical models to predict the shrinkage of concrete members. However, these models are not applicable for predicting the development of non-uniform shrinkage in the composite slab. The few experimental results available in the literature (Shayan *et al*. 2010, Gilbert *et al*. 2012, Al-deen *et al*. 2015) are not sufficient for the development of an empirical model.

In this context, this paper proposes a hydro-mechanical analysis method; capable of predicting the development of non-uniform shrinkage through the depth of the equivalent slab, which can be used in conjunction with other available models to predict the long-term behaviour of steel-concrete composite slabs. The performance of the proposed model is then validated against the experimental results.

2. The hydro-mechanical model

2.1 Overview of the model

Due to complex nature of the problem, the prediction of non-uniform shrinkage in the equivalent slab is achieved in a number of steps. The first step is to simulate the non-uniform drying of concrete in the equivalent slab which is directly related to moisture diffusion of concrete. A concrete moisture diffusion model is used to calculate the variation of concrete internal relative humidity, both in the time domain and space domain, through the thickness of the equivalent slab. In the second step, the result of the first phase is used to calculate the induced shrinkage strain of the equivalent slab due to its non-uniform drying. In the third phase, total shrinkage strain induced on the concrete is calculated. As concrete undergoes autogenous shrinkage, in addition to drying shrinkage, autogenous shrinkage strain is calculated and added to drying shrinkage strain to determine the total induced shrinkage strain. The cross-sectional rigidity of the concrete slab readjusts this non-linear drying shrinkage strain to a linear but non-uniform shrinkage strain. A simple mechanical model is proposed to simulate this readjustment in the final step. The flowchart of the calculation process is presented in Fig. 2.

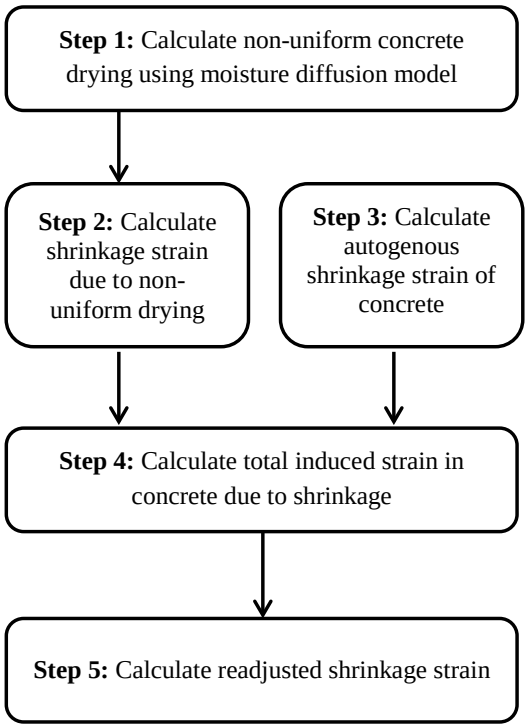

Fig. 2 Calculation process of the non-uniform shrinkage strain in the equivalent slab

2.2 Concrete moisture diffusion model

Over the years' considerable research have been conducted on the moisture diffusion behaviour of concrete and some mathematical models (Roy 1937, Bažant and Najjar 1971, Sakata 1983, Baroghel-Bouny *et al*. 1999, Benboudjema *et al*. 2005, Kwak *et al*. 2006, Moon 2006) with various degrees of complexities have been proposed describing this behaviour. For this study, a relatively simple model proposed by Moon (2006) was selected. The model is based on linear diffusion approach and enables the estimation of internal relative humidity (*RH*%) of the concrete slab both at time domain and space domain. The model can be mathematically described as follows

$$RH_{I,y,k} = RH_I - \left(RH_I - RH_S\right)\left[erfc\left(\frac{y}{2\sqrt{Dk}}\right)\right] \quad (1)$$

Here, k is the drying time, $RH_{I,y,k}$ is the internal relative humidity at a depth y from the drying surface. RH_I is the initial internal relative humidity and RH_S is the relative humidity of the drying surface. D is the ageing moisture diffusion coefficient of concrete and *erfc* is the complementary error function. The model assumes that the relative humidity of the drying surface (RH_S) remains constant throughout the drying process. The typical results from this model for both equivalent slab and a solid concrete slab are shown in Figs. 3(a) and (b).

2.3 Induced drying shrinkage strain

The internal relative humidity (i.e., pore pressure) could be used to predict the induced drying shrinkage strain in concrete (Bazant 1985). The internal relative humidity of the concrete estimated in the moisture diffusion model was used to calculate the induced drying shrinkage strain of the equivalent slab. The relationship between the induced shrinkage strain and relative humidity can be approximated for the case of high relative humidity (i.e., RH > 50%) as linearly proportional (Weiss and Shah 2002). As a result, the induced drying shrinkage strain of concrete at a distance "y" from the drying surface after time "k" from the start of drying, $\varepsilon_{sh,d,y,k}$, can be expressed by a constant free shrinkage coefficient ($\varepsilon_{sh,ult}$) and the change of relative humidity as presented in Eq. (2)

$$\varepsilon_{sh.d,y,k} = \varepsilon_{sh.ult}\left(1 - RH_{I,y,k}\right) \quad (2)$$

The constant free shrinkage coefficient ($\varepsilon_{sh.ult}$) can be considered as the slope of the induced drying shrinkage versus the change in the relative humidity relationship. The typical results from this stage for both equivalent slab and a solidconcrete slab are shown in Figs. 3(c) and (d).

2.4 Total induced strain due to shrinkage

Strain induced due to autogenous shrinkage should be added to the strain induced by concrete drying to estimate the total induced strain in concrete due to shrinkage. In this study, autogenous shrinkage strain was estimated following *fib*2010 ((fib) 2010) recommendations. It assumes that autogenous shrinkage strain is uniform throughout the depth of the slab but increases with time. The autogenous shrinkage ($\varepsilon_{sh.a,k}$) can be estimated using basic nominal shrinkage coefficient, ε_{sh0} and the time function, $\varepsilon_{bs,k}$ as illustrated in Eqs. (3)-(5)

$$\varepsilon_{sh.a,k} = \varepsilon_{sh.0}\,\beta_{bs,k} \quad (3)$$

Basic notional shrinkage coefficient ε_{sh0} is a function of the mean compressive strength of concrete, f_{cm} at the age of 28 days and can be expressed as

$$\varepsilon_{sh.0} = -\alpha_{bs}\left(\frac{0.1 f_{cm}}{6 + 0.1 f_{cm}}\right)^{2.5} \times 10^{-6} \quad (4)$$

Where α_{bs} is a coefficient, which depends on the type of the cement. Details of the model can be found in ((fib) 2010). The time function is expressed as

$$\beta_{bs,k} = 1 - e^{-0.2\sqrt{k}} \quad (5)$$

Once induced autogenous strain ($\varepsilon_{sh.a,k}$) is estimated it is added to the drying shrinkage strain ($\varepsilon_{sh.d,y,k}$) to calculate the total induced shrinkage strain ($\varepsilon_{sh.In,y,k}$)

$$\varepsilon_{sh.In,x,k} = \varepsilon_{sh.a,k} + \varepsilon_{sh.d,x,k} \quad (6)$$

The typical results from this stage for both equivalent slab and a solid concrete slab are shown in Figs. 3(e) and (f).

2.5 Readjusted shrinkage strain

As mentioned before, the cross-sectional rigidity of the equivalent slab will redistribute the induced shrinkage strain. Gilbert and Ranzi (2011) presented a rigorous analytical procedure for the time-dependent analysis of concrete cross-sections with uniform shrinkage through the thickness of the concrete slab using the age-adjusted effective modulus method (AEMM) (Dilger and Neville 1971, Bazant 1972). The algebraic formulation of the age-adjusted effective modulus method allows the solutions to be presented in closed form. The method is modified here to calculate the redistributed shrinkage strain by layering the concrete cross-section, with the shrinkage strain specified at the centroid of each concrete layer depending on its position within the cross-section.

A typical cross-section with m concrete layers is shown in Fig. 4. The thickness of the i^{th} concrete layer is t_i. The reference axis (the x-axis) is taken as the top surface of the concrete, and the positive direction of the transverse y-axis is as shown in Fig. 4.

The constitutive relationship for the i^{th} concrete layer at time "k" after the start of drying is expressed as

$$\sigma_{c(i),k} = \bar{E}_{e,k}\left[\left(\varepsilon_{r,sh,k} + y\kappa_{sh,k}\right) - \varepsilon_{sh(i),k}\right] \quad (7)$$

Where $\sigma_{c(i),k}$ is the stress of the i^{th} concrete layer, $\bar{E}_{e,k}$ is the age-adjusted effective modulus of the i^{th} concrete layer and $\varepsilon_{sh(i),k}$ is the induced shrinkage strain at the centroid of

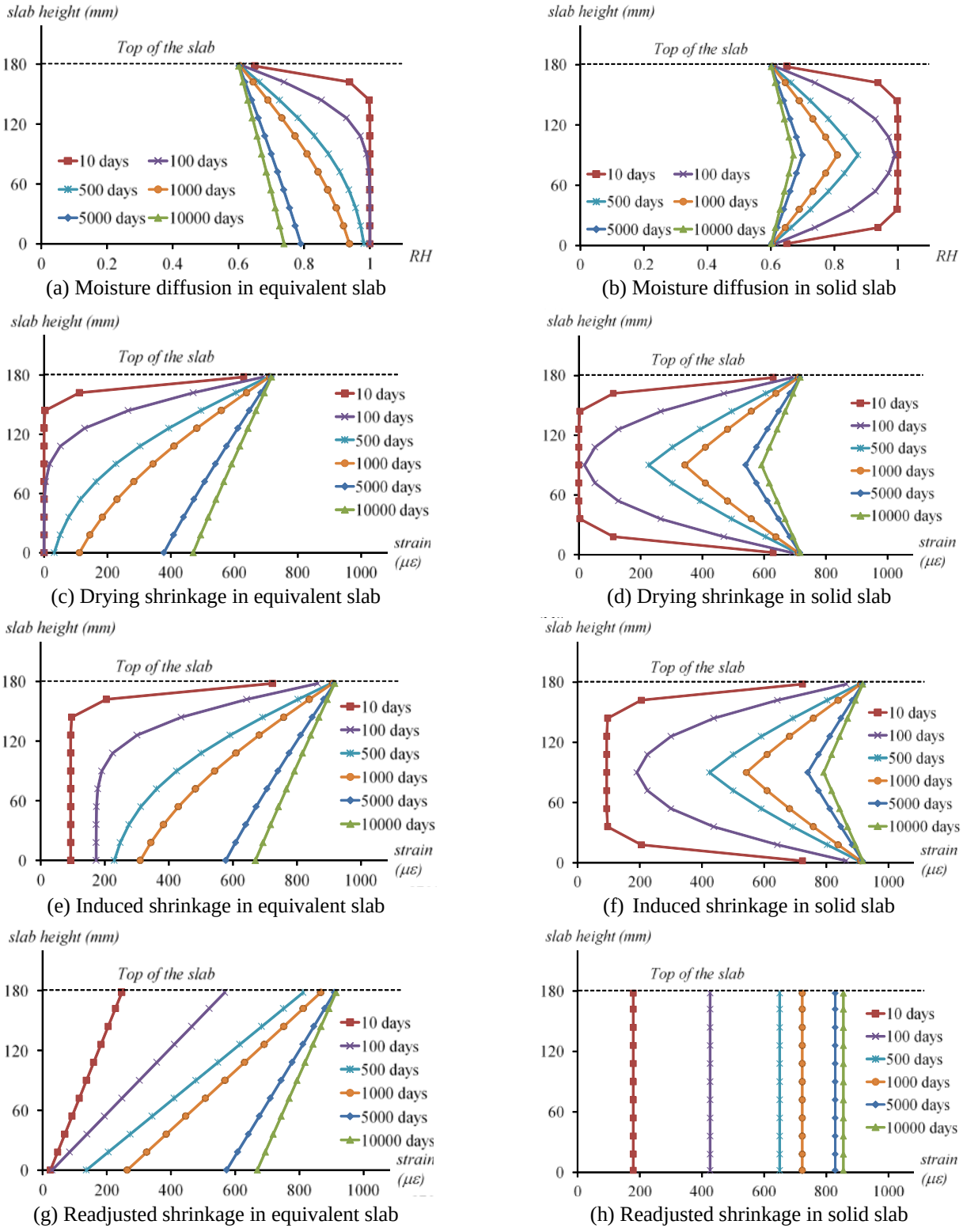

(a) Moisture diffusion in equivalent slab

(b) Moisture diffusion in solid slab

(c) Drying shrinkage in equivalent slab

(d) Drying shrinkage in solid slab

(e) Induced shrinkage in equivalent slab

(f) Induced shrinkage in solid slab

(g) Readjusted shrinkage in equivalent slab

(h) Readjusted shrinkage in solid slab

Fig. 3 Variation of moisture content and strain, at different stages of the calculation, through the depth of an equivalent slab and a solid slab at various days

the i^{th} concrete layer. The terms $\varepsilon_{r.sh,k}$ and $\kappa_{sh,k}$ are defined in Fig. 4(c) and the aim of the model described in this subsection is to determine values of $\varepsilon_{r.sh,k}$ and $\kappa_{sh,k}$.

The contribution of the i^{th} concrete layer to the internal axial force and moment at time "k" after the start of drying can be determined as

$$\begin{aligned} N_{c(i),k} &= \int_{A_{c(i)}} \sigma_{c(i),k}\, dA \\ &= \int_{A_{c(i)}} \overline{E}_{e,k}\left[\left(\varepsilon_{r,sh,k} + y\kappa_{sh,k}\right) - \varepsilon_{sh(i),k}\right] dA \\ &= A_{c(i)}\overline{E}_{e,k}\varepsilon_{r,sh,k} + B_{c(i)}\overline{E}_{e,k}\kappa_{sh,k} + A_{c(i)}\overline{E}_{e,k}\varepsilon_{sh(i),k} \end{aligned} \tag{8a}$$

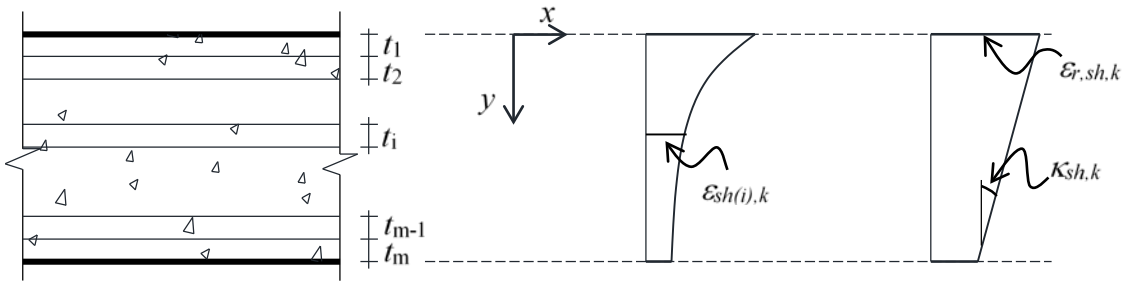

(a) Typical slab cross-section (b) Induced shrinkage strain (c) Readjusted shrinkage strain

Fig. 4 Generic cross-section and strain profiles considered in the numerical model for readjusted shrinkage strain

$$\begin{aligned} M_{c(i),k} &= \int_{A_{c(i)}} y\sigma_{c(i),k}\,dA \\ &= \int_{A_{c(i)}} y\overline{E}_{e,k}\left[\left(\varepsilon_{r,sh,k} + y\kappa_{sh,k}\right) - \varepsilon_{sh(i),k}\right]dA \\ &= B_{c(i)}\overline{E}_{e,k}\varepsilon_{r,sh,k} + I_{c(i)}\overline{E}_{e,k}\kappa_{sh,k} + B_{c(i)}\overline{E}_{e,k}\varepsilon_{sh(i),k} \end{aligned} \tag{8b}$$

Where $N_{c(i),k}$ and $M_{c(i),k}$ are the axial force resisted by the i^{th} concrete layer and the moment of the axial force about the x-axis, respectively. $A_{c(i)}$, $B_{c(i)}$ and $I_{c(i)}$ are the area of the i^{th} concrete layer and the first and second moments of area of the i^{th} concrete layer about the x-axis, respectively.

If $N_{e,k}$ and $M_{e,k}$ are the external axial force and moment applied to the cross-section, the equilibrium equations are therefore

$$\mathbf{r}_{e,k} = \mathbf{D}_{sh,k}\boldsymbol{\varepsilon}_{sh,k} - \mathbf{f}_{sh,k} \tag{9}$$

where

$$\mathbf{r}_{e,k} = \begin{bmatrix} N_{e,k} \\ M_{e,k} \end{bmatrix} \tag{10}$$

$$\mathbf{D}_{sh,k} = \overline{E}_{e,k}\begin{bmatrix} A_c & B_c \\ B_c & I_c \end{bmatrix} \tag{11}$$

$$\mathbf{f}_{sh,k} = \overline{E}_{e,k}\sum_{i=1}^{m}\begin{bmatrix} A_{c(i)} \\ B_{c(i)} \end{bmatrix}\varepsilon_{sh(i),k} \tag{12}$$

$$\boldsymbol{\varepsilon}_{sh,k} = \begin{bmatrix} \varepsilon_{r,sh,k} \\ \kappa_{sh,k} \end{bmatrix} \tag{13}$$

Since the equivalent slab is not subjected to any external load, both $N_{e,k}$ and $M_{e,k}$ are zero. Hence

$$\mathbf{r}_{e,k} = \begin{bmatrix} 0 \\ 0 \end{bmatrix} \tag{14}$$

Substituting this value in Eq. (9), we get

$$\boldsymbol{\varepsilon}_{sh,k} = \mathbf{D}_{sh,k}^{-1}\mathbf{f}_{sh,k} \tag{15}$$

This will provide the readjusted shrinkage distribution of the equivalent slab, which can be used to calculate the structural response of the composite slab due to non-uniform shrinkage. The typical results from this stage for both equivalent slab and a solid concrete slab are shown in Figs. 3(g) and (h).

This non-uniform shrinkage profile described in Eq. (15) is then used as an input for the mathematical model capable of predicting the response of the steel-concrete composite slab due to this shrinkage. The model is well documented in the literature (Ranzi *et al*. 2013a, Al-deen and Ranzi 2015, Al-deen *et al*. 2015).

3. Model validation for cross-sectional behaviour

3.1 Brief description of the experiments

Experiment results reported in (Al-deen and Ranzi 2015) is used to validate the mathematical model proposed in this paper. For the convenience of the reader, a brief description of those experiments is presented here. In the experiment, shrinkage behaviour of total twelve slabs was monitored for four months. Based on the presence of the steel deck and the drying conditions of the slab surfaces, four different types of slabs were used with three slabs of the same type. Out of the four types, two types of specimens were cast without any steel deck while the other two had profiled steel sheeting at the bottom. The two categories of specimens without any steel decking differed in terms of drying condition. One type referred as "SS" type consisted of a solid concrete slab with both top and bottom faces exposed to the environment so that that moisture can egress from both faces. The other type, referred as "SP", was identical to type "SS" with the only difference that the bottom face of the slab was sealed using a plastic sheet. The

Table 1 Geometric properties of Condeck HP and PrimeForm profiles (per metre width)

Profiles sheeting (thickness)	Cross-sectional area (mm^2)	Level of the centroid of the steel deck from its bottom face (mm)
Condeck HP (0.75 mm)	1211	15.39
PrimeForm (0.6 mm)	940	15.8

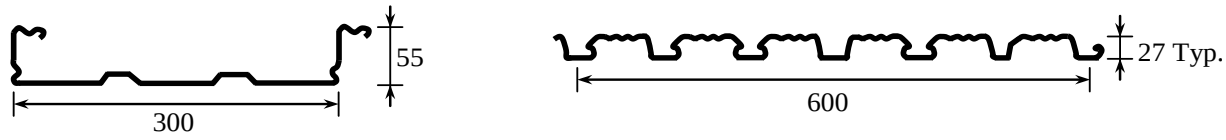

(a) Condeck HP profile used in CK type specimens (b) PrimeForm profile used in PF type specimens

Fig. 5 Details of the Condeck HP and PrimForm steel deck profiles

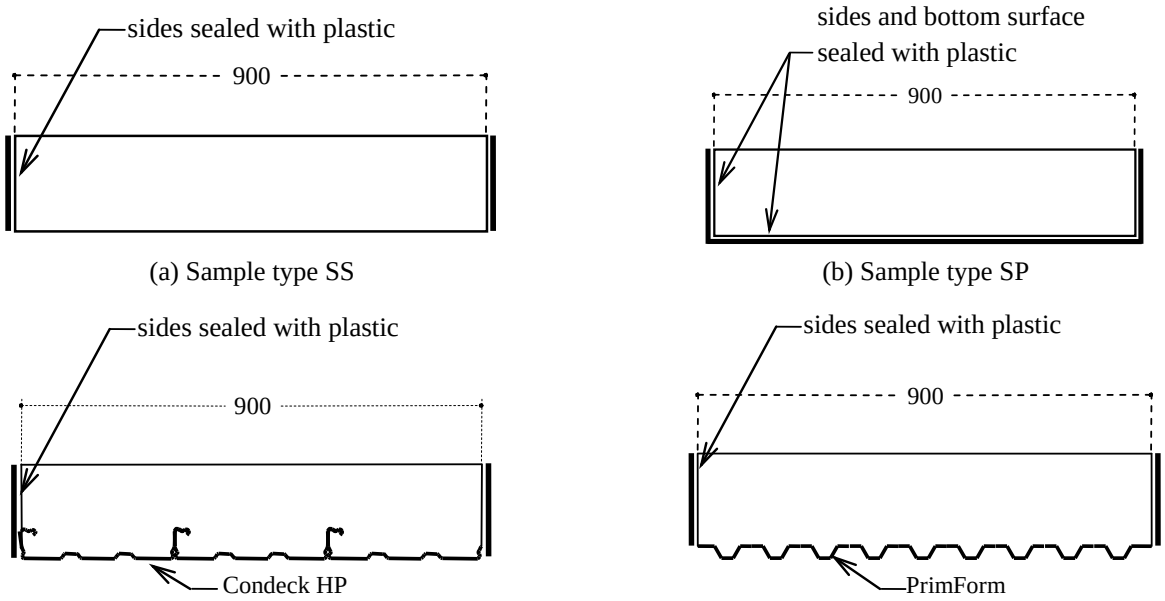

(a) Sample type SS (b) Sample type SP

(c) Sample type CK (d) Sample type PF

Fig. 6 Details of the slab specimens used in the experiments presented in (Al-deen and Ranzi 2015)

Table 2 Details of slab specimens presented in Al-deen and Ranzi (2015)

Specimen ID	Dimensions of slab samples (mm × mm × mm)	Exposed conditions of top and bottom slab surfaces
SS120	900 × 900 × 120	Top and bottom exposed
SS180	900 × 900 × 180	Top and bottom exposed
SS250	900 × 900 × 250	Top and bottom exposed
SP120	900 × 900 × 120	Top exposed and bottom sealed with plastic
SP180	900 × 900 × 180	Top exposed and bottom sealed with plastic
SP250	900 × 900 × 250	Top exposed and bottom sealed with plastic
PF120	900 × 900 × 120	Top exposed and bottom sealed by the presence of the PrimForm steel sheeting
PF180	900 × 900 × 180	Top exposed and bottom sealed by the presence of the PrimForm steel sheeting
PF250	900 × 900 × 250	Top exposed and bottom sealed by the presence of the PrimForm steel sheeting
CK120	900 × 900 × 120	Top exposed and bottom sealed by the presence of the Condeck HP steel sheeting
CK180	900 × 900 × 180	Top exposed and bottom sealed by the presence of the Condeck HP steel sheeting
CK250	900 × 900 × 250	Top exposed and bottom sealed by the presence of the Condeck HP steel sheeting

*Note: all slab edges are sealed with plastic

presence of the plastic sheet prevented the moisture from egressing from the bottom of the slab, similar to steel decking, without the restraining action of the deck. The specimens with steel decking differed in terms of decking used as one type denoted as “CK” used 0.75 mm Condeck HP® while the other type referred as “PF”, used 0.6 mm PrimeForm® steel sheeting. These steel decking prevented moisture egress from the bottom of the slab and provided an eccentric restraint to the slab. The details of the Condeck HP and PrimeForm profiles are presented in Fig. 5, and their geometric properties are tabulated in Table 1. Each type of slab had one specimen with 120 mm, one with

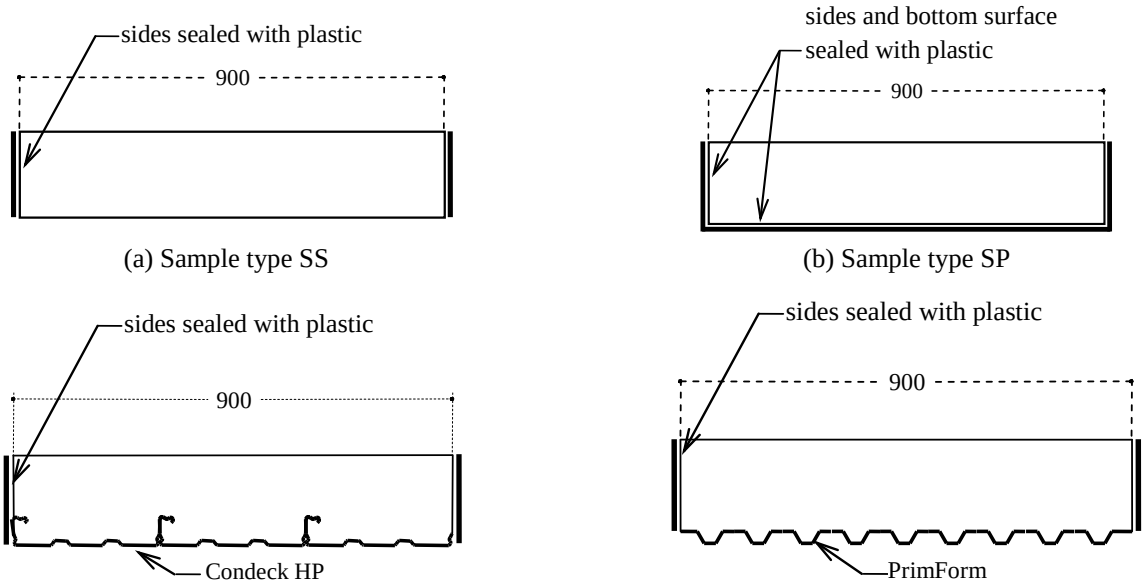

(a) Sample type SS (b) Sample type SP

(c) Sample type CK (d) Sample type PF

Fig. 6 Details of the slab specimens used in the experiments presented in (Al-deen and Ranzi 2015)

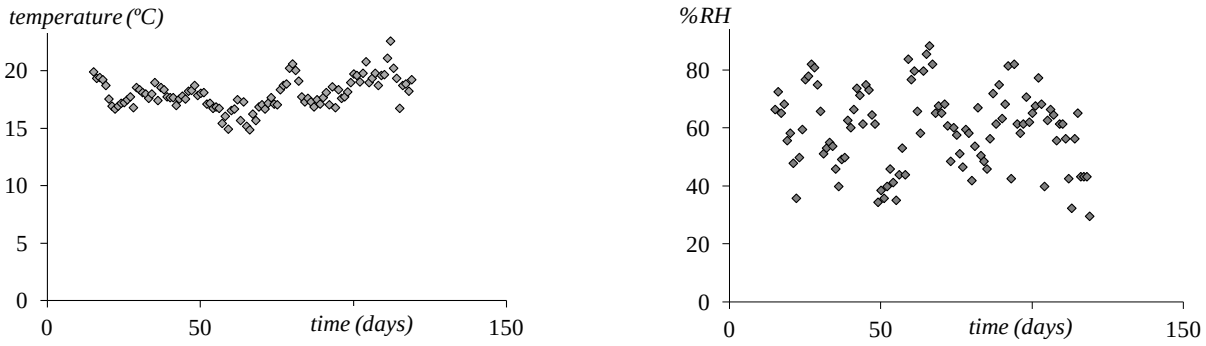

(a) Temperature (b) Relative humidity

Fig. 7 Measured daily ambient temperature and relative humidity of the experiments presented in Al-deen and Ranzi (2015)

180 mm and one with 250 mm depth. The length and width of all the specimens were 900 mm. The samples were cast without any additional reinforcement and maintained unloaded to monitor shrinkage effects only. The cross-sections of different types of specimens used in the experiment are shown in Fig. 6, and their details are summarised in Table 2. In a real floor system, moisture cannot egress from the side of the slabs due to continuities of the slab. Therefore, to prevent moisture egress from the side of the specimens, their side edges were sealed with plastic.

Same batch of concrete was used to cast all the specimens, and they were moist cured for 15 days after casting. After that, the curing was stopped, and the long-term behaviour of the specimens due to shrinkage was monitored using strain gauges. The specimens were cast horizontally. However, to facilitate deformation without any restraint, these specimens were placed vertically on top of three rollers after three days of casting. To ensure all the specimens were subjected to a very similar environmental condition, they were placed very close to each other. Ambient temperature and relative humidity were recorded for the entire duration of the long-term tests, and daily average values are reported in Fig. 7.

3.2 Comparison of cross-sectional behaviour with experimental results

For simulating the experiments using the proposed analysis method, a simplifying assumption was made. The proposed model uses a constant external relative humidity (RH_S in Eq. (1)). The measurement of relative humidity of the experimental environment (Fig. 7(b)) shows that it varied significantly during the experiment. For the calculation presented in this section, it was assumed that in the experiments the external relative humidity was constant and was equal to the average relative humidity of the total duration of the experiments. Two of the inputs required for the proposed model, the ageing moisture diffusion coefficient of concrete (D) in Eq. (1) and constant free shrinkage coefficient ($\varepsilon_{sh,ult}$) in Eq. (2) were not measured in the experiments. For the calculations, their values were calibrated against the measurement results of specimens SS120, SS180 and SS250. These calibrated values were

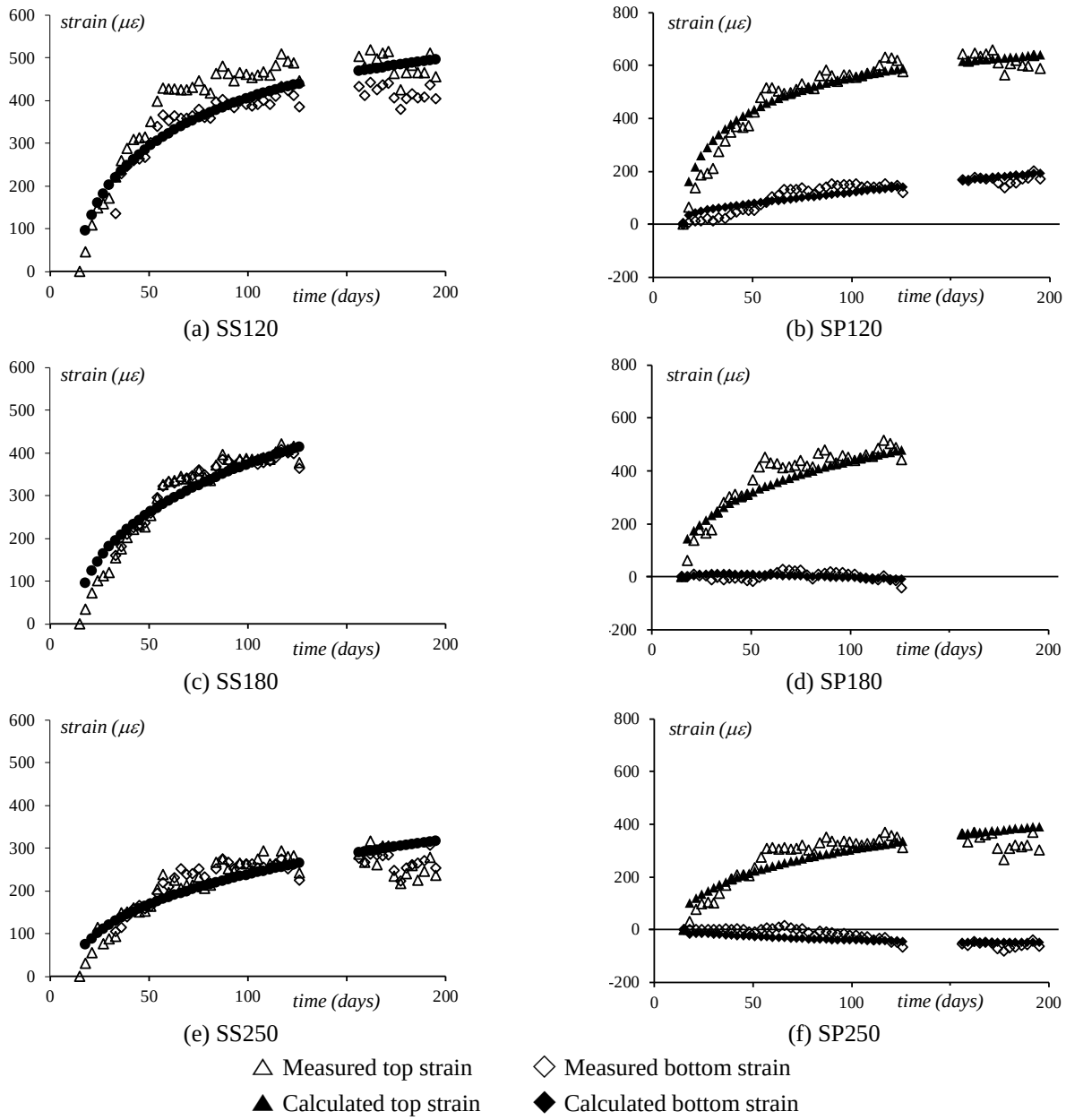

Fig. 8 Comparison between measured and calculated strains for sample types SS and SP

then used for rest of the calculations for model validation. The comparison between the measured strain of "SS" and "SP" type slabs and calculated strain using the proposed model is presented in Fig. 8. The results of the "SP" type slabs show that the proposed model can predict the top and bottom strain of the slab reasonably well. As slab types "CK" and "PF" are a steel-concrete composite slab, their strains were calculated using the proposed model in conjunction with the model presented in (Al-deen *et al.* 2015). To be consistent, sign convention for strain calculation presented in (Al-deen *et al.* 2015) was also used in this paper. The comparison between measured and calculated strains of "CK" and "PF" type slabs are shown in Fig. 9. Again, the comparison between measured and calculated curvatures of CK" and "PF" type slabs are shown in Fig. 10. From these figures in can be seen that the calculated results using the proposed model are in good agreement with the measured values. As the relative humidity of the environment of the experiment room was varied considerably during the experiment, the strain and curvature measurement values also fluctuated with time. These fluctuations were not captured in the calculated values as it assumed constant external relative humidity. Regardless of this inconsistency, the proposed model can predict the cross-sectional behaviour due to non-uniform shrinkage with an acceptable level of accuracy.

4. Model validation for slab deflection

The experimental results on shrinkage deflection of simply supported steel-concrete composite slabs are reported in (Al-deen *et al.* 2015). The details of the specimen cross-section and test setup of these experiments

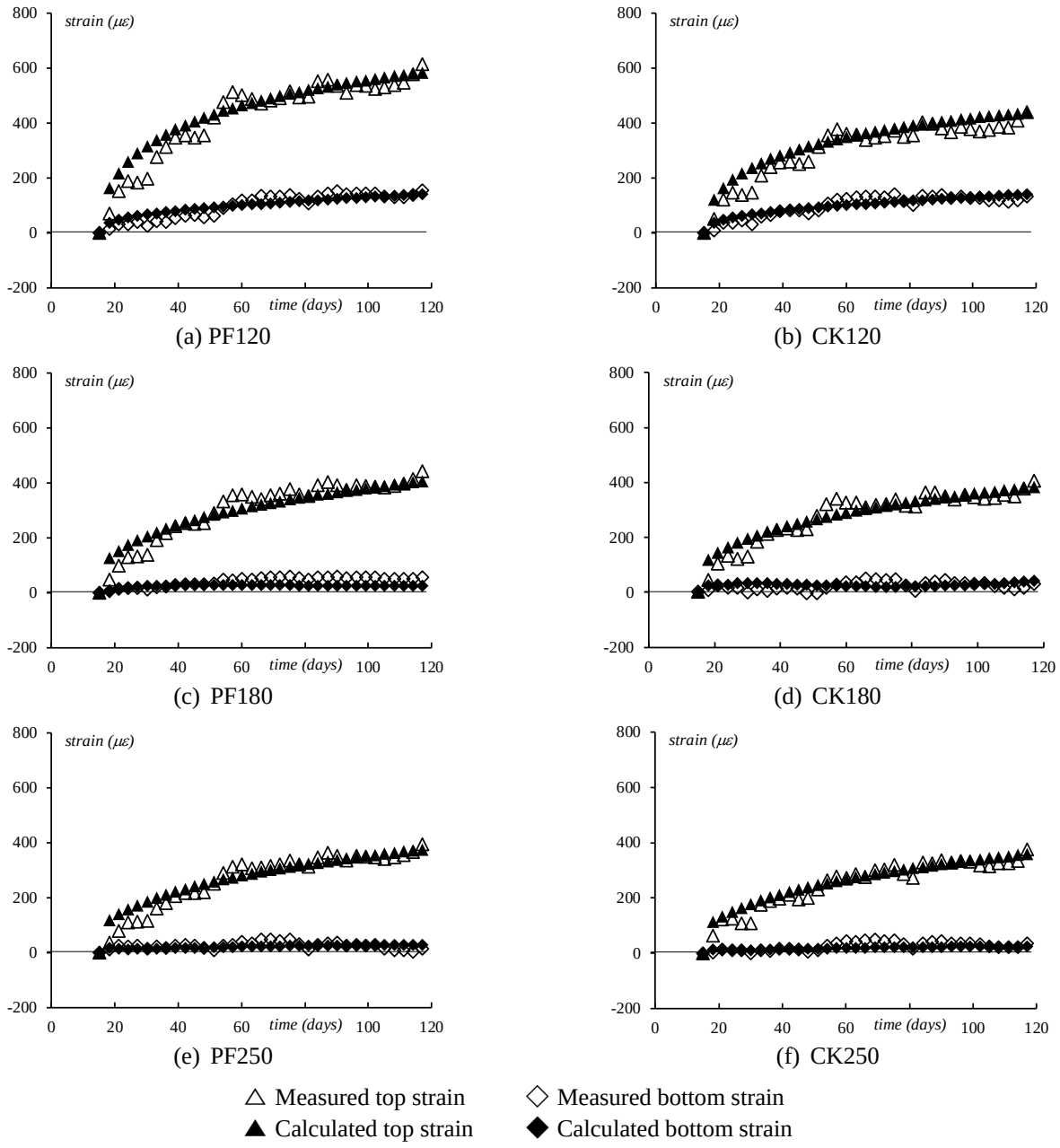

Fig. 9 Comparison between measured and calculated strains for sample types SS and SP

are shown in Fig. 11. These experimental results were used to examine the accuracy of the proposed model on predicting the long-term deflection of steel-concrete composite slabs. To calculate the slab deflection at first, the strain distribution at the various cross-sections along the length of the slab was calculated using the same method described in the previous section.

From the strain distribution, the curvatures of the cross-sections were obtained, which was then used in member analysis to calculate the slab deflection. The member analysis at times k_0 and k were performed considering the deflected shape to vary along the member with a shape described by a fourth-order polynomial. Based on this assumption, the mid-span deflections were determined based on the curvature values calculated at mid-span and the ends of the slab: (Gilbert and Ranzi 2011)

$$v_j = \frac{L^2}{96}\left(\kappa_{(z=0),j} + 10\kappa_{(z=L/2),j} + \kappa_{(z=L),j}\right) \tag{16}$$

where the subscript '*j*' equals '0' for the instantaneous analysis and '*k*' for the long-term one, v_j represents the midspan vertical deflection of the slab at time k_j. L depicts the span of the slab, z is the coordinate along the member length, while $\kappa_{(z=0),j}$, $\kappa_{(z=L/2),j}$ and $\kappa_{(z=L),j}$ define the curvature values calculated at time k_j from the cross-sectional calculations at the two ends and mid-span of the slab. The comparison between the measured slab deflections and calculated deflection using the proposed model is presented in Fig. 12. This comparison clearly shows that the proposed model can predict the long-term shrinkage deflection of steel-concrete composite slab reasonably accurately. Again,

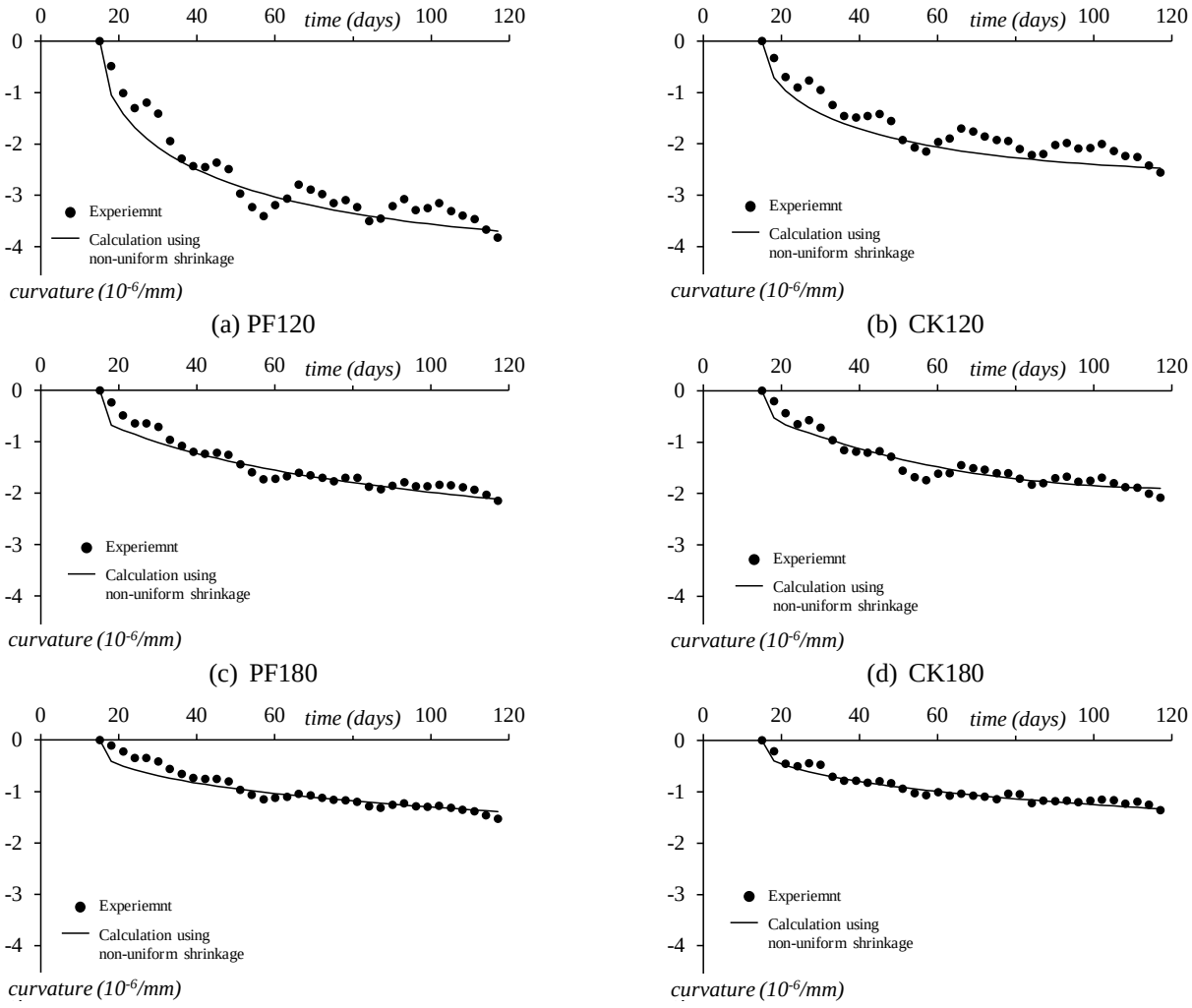

Fig. 10 Comparisons between numerical measurements and calculated values for the slab curvature

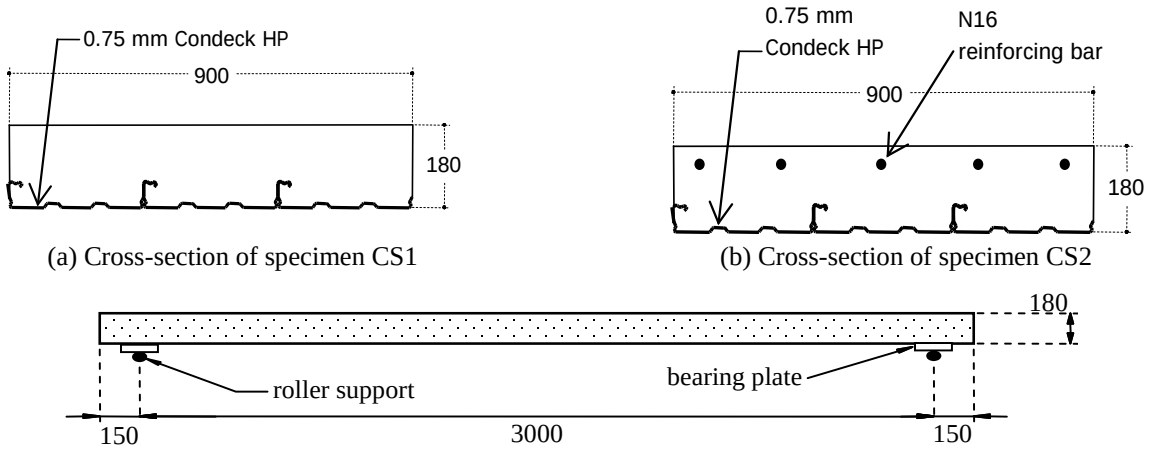

Fig. 11 Cross sections and test setup (dimensions are in mm) of the experiment presented in (Al-deen et al. 2015)

the fluctuations of slab deflection due to changes in external relative humidity were not captured by the proposed model as it assumed constant external relative humidity. However, the proposed model can describe the long-term behaviour of composite slab due to non-uniform shrinkage at sufficient level of accuracy that it can be used for regular design calculations.

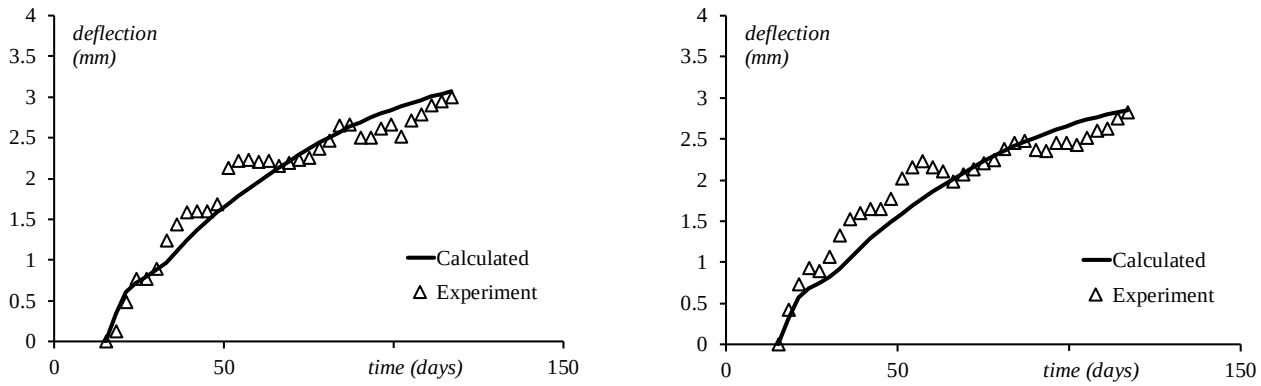

(a) Cross-section of specimen CS1 (b) Cross-section of specimen CS2

Fig. 12 Comparisons between the experimental data (Al-deen *et al*. 2015) and the numerical results calculated with the proposed method

5. Conclusions

This paper proposed a multi-step hydro-mechanical analysis method for predicting the development of non-uniform shrinkage through the depth of the steel-concrete composite slab. It also demonstrated how this proposed method could be used in conjunction with previously proposed structural analysis model to calculate the effect of this non-uniform shrinkage on the long-term behaviour of composite slabs. In the proposed analysis method, concrete moisture diffusion model was used to simulate the non-uniform drying of composite slab. Mechanical models were then used to calculate resulting shrinkage strain from non-uniform drying and its effect on the long-term behaviour of the composite slabs. The performance of the analysis method was investigated by comparing with the experimental results. The comparison showed that the analysis results could describe the cross-sectional strain and member deflection behaviour reasonably accurately. This demonstrates that the proposed hydro-mechanical analysis method can be used in conventional design for calculating the long-term deflection of composite slabs.

References

Abdullah, R. and Easterling, S.W. (2009), "New evaluation and modeling procedure for horizontal shear bond in composite slabs", *J. Constr. Steel Res.*, **65**(4), 891-899.

(fib), I.F.f.S.C. (2010), *fib Model Code for Concrete Structures 2010*, Ernst & Sohn.

Airumyan, E., Belyaev, V. and Rumyancev, I. (1990), "Efficient embossment for corrugated steel sheeting", *Proceedings of IABSE Symposium on Mixed Structures Including New Materials*, Brussels, Belgium, September.

Al-deen, S. and Ranzi, G. (2015), "Effects of non-uniform shrinkage on the long-term behaviour of composite steel-concrete slabs", *Int. J. Steel Struct.*, **15**(2), 415-432.

Al-deen, S., Ranzi, G. and Vrcelj, Z. (2011a), "Full-scale long-term and ultimate experiments of simply-supported composite beams with steel deck", *J. Constr. Steel Res.*, **67**(10), 1658-1676.

Al-deen, S., Ranzi, G. and Vrcelj, Z. (2011b), "Full-scale long-term experiments of simply supported composite beams with solid slabs", *J. Constr. Steel Res.*, **67**(3), 308-321.

Al-deen, S., Ranzi, G. and Uy, B. (2015), "Non-uniform shrinkage in simply-supported composite steel-concrete slabs", *Steel Compos. Struct., Int. J.*, **18**(2), 375-394.

Al-Deen, S., Ranzi, G. and Vrcelj, Z. (2012), "Long-term experiments of composite beams and connections", *Mag. Concrete Res.*, **64**(9), 849-861.

Alsamsam, I. (1991), *Serviceability Criteria for Composite Floor Systems*, The University of Minnesota, MN, USA.

AS2327.1 (2003), Composite structures – Part 1: Simply Supported Beams; Standards Australia, Sydney.

Baroghel-Bouny, V., Mainguy, M., Lassabatere, T. and Coussy, O. (1999), "Characterization and identification of equilibrium and transfer moisture properties for ordinary and high-performance cementitious materials", *Cement Concrete Res.*, **29**(8), 1225-1238.

Bazant, Z.P. (1972), "Prediction of concrete creep effects using age-adjusted effective modulus method", *ACI J.*, **69**(4), 212-217.

Bazant, Z.P. (1985), *Fourth RILEM International Symposium on Creep and Shrinkage of Concrete: Mathematical Modeling*.

Bažant, Z.P. and Najjar, L.J. (1971), "Drying of concrete as a nonlinear diffusion problem", *Cement Concrete Res.*, **1**(5), 461-473.

Benboudjema, F., Meftah, F. and Torrenti, J.M. (2005), "Interaction between drying, shrinkage, creep and cracking phenomena in concrete", *Eng. Struct.*, **27**(2), 239-250.

Bradford, M.A. (2010), "Generic modelling of composite steel-concrete slabs subjected to shrinkage, creep and thermal strains including partial interaction", *Eng. Struct.*, **32**(5), 1459-1465.

Bradford, M.A. and Gilbert, R.I. (1991), "Time-dependent behaviour of simply-supported steel-concrete composite beams", *Mag. Concrete Res.*, **43**(157), 265-274.

Chen, S. and Shi, X. (2011), "Shear bond mechanism of composite slabs — A universal FE approach", *J. Constr. Steel Res.*, **67**(10), 1475-1484.

Chen, S., Shi, X. and Qiu, Z. (2011), "Shear bond failure in composite slabs – A detailed experimental study", *Steel Compos. Struct., Int. J.*, **11**(3), 233-250.

Crisinel, M. and Marimon, F. (2004), "A new simplified method for the design of composite slabs", *J. Constr. Steel Res.*, **60**(3-5), 481-491.

Daniels, B.J. and Crisinel, M. (1993), "Composite slab behavior and strength analysis. Part II: Comparisons with test results and parametric analysis", *J. Struct. Eng.*, **119**(1), 36-49.

Dilger, W. and Neville, A.M. (1971), "Method of creep analysis of structural members", *Special Publication*, **27**, 349-372.

Easterling, W.S. and Young, C.S. (1992), "Strength of composite slabs", *J. Struct. Eng.*, **118**(9), 2370-2389.

Eldib, M.A., Maaly, H.M., Beshay, A.W. and Tolba, M.T. (2009), "Modelling and analysis of two-way composite slabs", *J. Constr. Steel Res.*, **65**(5), 1236-1248.

Eurocode 4 (2004), EC4 Design of composite steel and concrete structures – Part 1.1: General rules and rules for buildings; British Standards Institution.

Fan, J., Nie, J., Li, Q. and Wang, H. (2010), "Long-term behavior of composite beams under positive and negative bending. I: experimental study", *J. Struct. Eng.*, **136**(7), 849-857.

Gholamhoseini, A., Gilbert, R.I., Bradford, M.A. and Chang, Z.T. (2012), "Long-term deformation of composite slabs", *Concrete in Australia*, **38**(4), 25-32.

Gilbert, R.I. (2013), "Time-dependent stiffnes of cracked reinforced and composite concrete slabs", *Proceedings of the 11th International Conference on Modern Building Materials, Structures and Techniques* (*MBMST*), Vilnius, Lithuania, May.

Gilbert, R.I. and Ranzi, G. (2011), *Time-Dependent Behaviour of Concrete Structures*, Spon Press, London, UK.

Gilbert, R.I., Bradford, M.A., Gholamhoseini, A. and Chang, Z.T. (2012), "Effects of shrinkage on the long-term stresses and deformations of composite concrete slabs", *Eng. Struct.*, **40**, 9-19.

Jeong, Y.-J., Kim, H.-Y. and Kim, S.-H. (2005), "Partial-interaction analysis with push-out tests", *J. Constr. Steel Res.*, **61**(9), 1318-1331.

Johnson, R.P. (1987), "Shrinkage induced curvature in composite beams with a cracked concrete flange", *Struct. Eng.*, **65B**(4), 72-76.

Kim, H.-Y. and Jeong, Y.-J. (2010), "Ultimate strength of a steel–concrete composite bridge deck slab with profiled sheeting", *Eng. Struct.*, **32**(2), 534-546.

Kwak, H.-G., Ha, S.-J. and Kim, J.-K. (2006), "Non-structural cracking in RC walls: Part I. Finite element formulation", *Cement Concrete Res.*, **36**(4), 749-760.

Lopes, E. and Simões, R. (2008), "Experimental and analytical behaviour of composite slabs", *Steel Compos. Struct., Int. J.*, **8**(5), 361-388.

Marimuthu, V., Seetharaman, S., Arul Jayachandran, S., Chellappan, A., Bandyopadhyay, T.K. and Dutta, D. (2007), "Experimental studies on composite deck slabs to determine the shear-bond characteristic values of the embossed profiled sheet", *J. Constr. Steel Res.*, **63**(6), 791-803.

Moon, J.H. (2006), *Shrinkage, Residual Stress and Cracking in Heterogeneous Material*, Purdue University, West Lafayette, IN, USA.

Patrick, M. and Bridge, R.Q. (1994), "Partial shear connection design of composite slabs", *Eng. Struct.*, **16**(5), 348-362.

Porter, M.L. (1985), "Analysis of two-way acting composite", *J. Struct. Eng.*, **111**(1), 1-18.

Porter, M.L. and Ekberg Jr., C.E. (1977), "Behavior of steel-deck-reinforced slabs", *J. Struct. Div.*, **103**(3), 663-677.

Ranzi, G. and Vrcelj, Z. (2009), "Closed form solutions for the long-term analysis of composite steel-concrete members subjected to non-uniform shrinkage distributions", *Proceedings of the 6th International Conference on Advances in Steel Structures*, Hong Kong, December.

Ranzi, G., Al-Deen, S., Ambrogi, L. and Uy, B. (2013a), "Long-term behaviour of simply-supported post-tensioned composite slabs", *J. Constr. Steel Res.*, **88**, 172-180.

Ranzi, G., Al-deen, S., Hollingum, G., Hone, T., Gowripalan, S. and Uy, B. (2013b), "An experimental study on the ultimate behaviour of simply-supported post-tensioned composite slabs." accepted for publication", *J. Constr. Steel Res.*, **89**, 293-306.

Ranzi, G., Leoni, G. and Zandonini, R. (2013c), "State of the art on the time-dependent behaviour of composite steel–concrete structures", *J. Constr. Steel Res.*, **80**, 252-263.

Roll, F. (1971), "Effects of differential shrinkage and creep on a composite steel-concrete structure", *ACI Special Publication*, **SP-27**(8), 187-214.

Roy, W.C. (1937), "Drying shrinkage of large concrete members", *J. Proceedings*, **33**(1), 327-336.

Sakata, K. (1983), "A study on moisture diffusion in drying and drying shrinkage of concrete", *Cement Concrete Res.*, **13**(2), 216-224.

Seres, N. and Dunai, L. (2011), "Experimental and numerical studies on concrete encased embossments of steel strips under shear action for composite slabs with profiled steel decking", *Steel Compos. Struct., Int. J.*, **11**(1), 39-58.

Shayan, S., Al-deen, S., Ranzi, G. and Vrcelj, Z. (2010), *Long-Term Behaviour of Composite Steel Concrete Slabs: An Experimental Study*, Sydney, Australia.

Stark, J.W.B. and Brekelmans, J.W.P.M. (1990), "Plastic design of continuous composite slabs", *J. Constr. Steel Res.*, **15**(1-2), 23-47.

Veljkovic, M. (1996), *Behaviour and Resistance of Composite Slabs*, Lulea University of Technology, Lulea, Sweden.

Veljković, M. (1998), "Influence of load arrangement on composite slab behaviour and recommendations for design", *J. Constr. Steel Res.*, **45**(2), 149-178.

Weiss, W.J. and Shah, S.P. (2002), "Restrained shrinkage cracking: the role of shrinkage reducing admixtures and specimen geometry", *Mater. Struct.*, **35**(2), 85-91.

Wright, H.D., Vitek, J.L. and Rakib, S.N. (1992), "Long-term creep and shrinkage in composite beams with partial connection", *ICE Proceedings, Struct. Build.*, **94**(2), 187-195.

CC